Japanese Journal of Applied Physics

The Japan Society of Applied Physics

Graphene Based Nanogenerator for Energy Harvesting

To cite this article: Junggou Kwon *et al* 2013 *Jpn. J. Appl. Phys.* **52** 06GA02

View the article online for updates and enhancements.

You may also like

- Fabrication of an Ultra-Flexible ZnO Nanogenerator for Harvesting Energy from Respiration
Hung-I Lin, Dong-Sing Wuu, Kun-Ching Shen et al.
- From contact electrification to triboelectric nanogenerators
Zhong Lin Wang
- Circumgalactic Medium at High Halo Masses—Signatures of Cold Gas Depletion in Luminous Red Galaxies
Marijana Smailagi, Jason Xavier Prochaska, Joseph Burchett et al.

This content was downloaded from IP address 18.217.73.187 on 24/04/2024 at 01:15

Japanese Journal of Applied Physics **52** (2013) 06GA02 **REVIEW PAPER**
http://dx.doi.org/**10.7567/JJAP.52.06GA02**

Graphene Based Nanogenerator for Energy Harvesting

Junggou Kwon[1], Bhupendra K. Sharma[2], and Jong-Hyun Ahn[2]*

[1]*SKKU Advanced Institute of Nanotechnology (SAINT), Sungkyunkwan University, Suwon, Gyeonggi 440-746, Republic of Korea*
[2]*School of Electrical and Electronic Engineering, Yonsei University, Seoul 120-749, Republic of Korea*
E-mail: ahnj@yonsei.ac.kr

Received November 23, 2012; accepted April 4, 2013; published online June 20, 2013

Development of energy harvesting system becomes one of the most important necessities of today. In this context, nanogenerators (NGs) have attracted considerable attentions in recent years due to their potential applications such as self-powered portable devices. This review article addresses the significant development of NGs systems based on semiconducting and insulating piezoelectric materials. Further, the need of mechanical flexibility and optical transparency on the demand of various electronic applications has been highlighted. In addition, we discussed some recent studies on graphene-based NGs which have been explored for stable performance of NGs.
© 2013 The Japan Society of Applied Physics

1. Introduction

Piezoelectric materials are smart materials that can convert mechanical energy from, for example, wind and flowing water into useful electric energy for portable electronic devices that require small power.[1–5)] In addition, this property has been harnessed sources of human-body motions such as heart beat,[6)] breathing and muscle movement to operate biomedical electronic devices,[7,8)] including pace maker and insulin delivery pump, for regulating body functions.[9,10)] For these systems, nanogenerators (NGs) have been developed on the basis of nanoscale piezoelectric materials for effective power generation.[11,12)] Among various piezoelectric materials, one-dimensional piezoelectric semiconductor materials with wurtzite structure such as ZnO, CdS, and GaN have been intensively studied and demonstrated in prototype devices.[13–17)] As an alternative, $PbZr_{0.52}Ti_{0.48}O_3$ (PZT) and poly(vinlyidene fluoride) (PVDF) with electromechanical coupling are a good traditional piezoelectric material with a larger piezoelectric constant as compared to that of piezoelectric semiconductor materials.[18–21)] These materials can be fabricated using relatively easy and low cost methods — a direct printing of high-quality, bulk PZT thin films on the wafers onto plastic substrates, and an electrospinning and a solution casting that PVDF nanofiber or film can be directly printed on the substrate.[22)] The great performance of PZT nanoribbon and PVDF nanofiber printed to flexible substrates suggests the possibility of various applications in portable and implantable electronic devices.[23)]

One of the big challenges of piezoelectric material-based nanogenerators is the short life time that limits their practical applications due to the poor mechanical properties of inorganic piezoelectric and metal electrode materials used as current collector. In addition, the opaque property of electrode materials is one of the significant hurdles to apply these NGs to new future applications including touch screen[24,25)] and wearable skin sensor[26,27)] that require optical transparency. To overcome such issues, carbon-based materials such as carbon nanotube and graphene films, that possess outstanding mechanical and optical properties have been integrated with piezoelectric NG because they can offer unique benefit in high-performance flexible and transparent devices.[28–35)] The resulting NG combined with carbon-based electrodes exhibits good mechanical bendability and optical transmittance.[36)]

In this article, we review recent progress in research on piezoelectric material based NG with particular focus on techniques for fabricating the flexible devices. After discussing function and fabrication of piezoelectric materials for nanogenerator, we highlight general approaches to the integration of these materials with graphene films on flexible substrates.

2. An Approach towards State-of-the-Art Piezoelectricity: Nanogenerator

There are various kinds of materials such as semiconducting piezoelectric, insulating piezoelectric, insulating polymeric piezoelectric, which have been used for demonstrating the NGs. ZnO, a semiconducting piezoelectric material, has been extensively investigated among all class of NG materials for a wide range of applications including electronic, optoelectronic, solar cells and piezoelectric NGs owing its excellent optical and electrical properties and the ability to control the synthesis of various ZnO nanostructures such as nanoparticles, nanowires, nanorods, nanobelts, nanotubes, and other complex forms.[37,38)] Wang and Song took the first step in the development of NGs using the piezoelectricity of aligned ZnO nanowires (NWs) with the help of atomic force microscopy (AFM).[39)] ZnO NWs were grown on *c*-plane oriented α-Al_2O_3 substrate by vapor–liquid–solid (VLS) process. Figure 1(a) shows the scanning electron microscopy (SEM) image of vertically aligned ZnO NWs. A continuous ZnO thin film is formed on substrate due to epitaxial relation between ZnO and α-Al_2O_3 which can be used as large electrode in transport measurement. Silver paste was attached to ZnO film on the substrate for the electric contact at the bottom of the NWs. Pt-coated Si tip attached in AFM, under the contact mode, was scanned over the top of ZnO NWs with a constant normal force of 5 nN between the tip and the sample surface. As the tip scanned over the vertically aligned NWs, the NWs were bent and, then the output voltages for each contact were measured as shown in Fig. 1(b). The output voltage was only observed when the maximum deflection occurs and it dropped to zero after relaxing the NW. The mechanism of creating the piezoelectric energy can be understood in terms of coupling between piezoelectric and semiconducting properties of ZnO. When AFM tip deflects the vertically aligned ZnO NW, its outer surface gets stretched (positive strain), while inner surface gets com-

© 2013 The Japan Society of Applied Physics

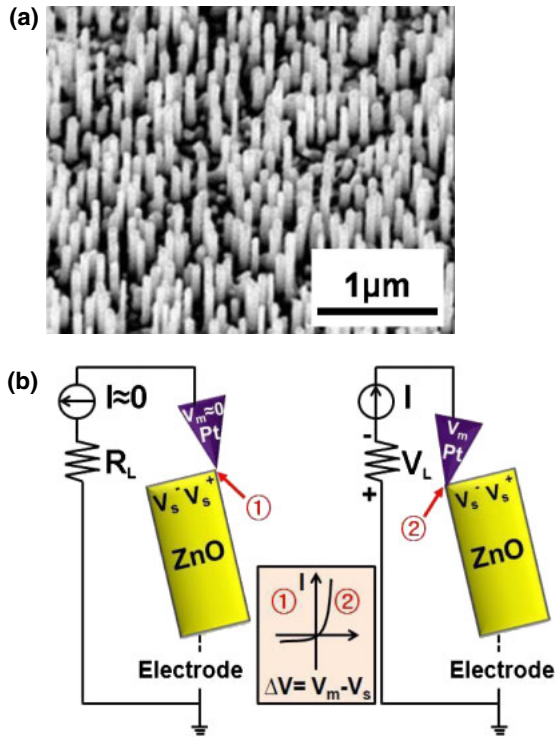

Fig. 1. (Color online) (a) SEM image of vertically aligned ZnO NWs. (b) Schematic representation of measurement of output voltage due to the bending of ZnO NW during the scanning of AFM tip over NWs.[39]

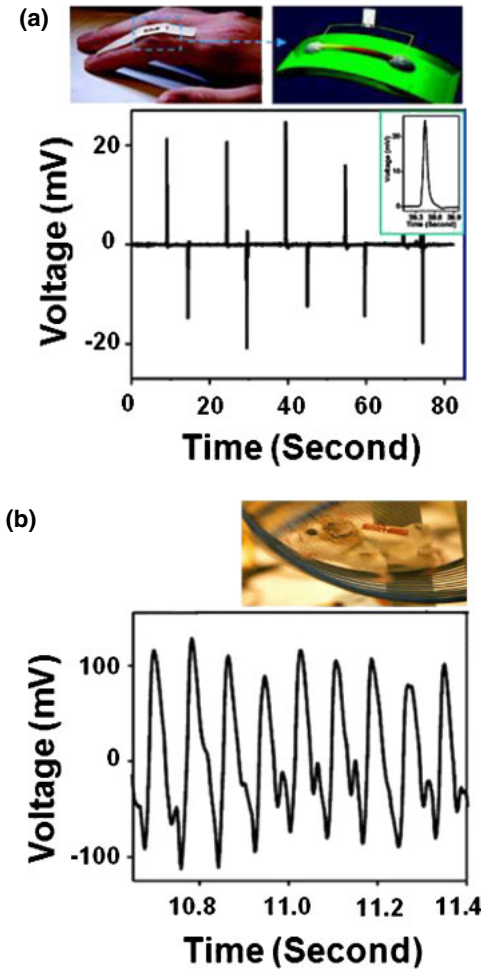

Fig. 2. (Color online) Photographs and electrical outputs generated from (a) finger tapping and (b) hamster movement by employing the ZnO based NGs.[40]

pressed (negative strain) and an electric field is created along the axis (z-axis) of NW due to the relative displacement of the Zn^{2+} cations with the respect to the O^{2-} anions as a consequence of piezoelectric effect in the wurtzite crystal structure. The direction of the electric field is parallel to the z-axis at the outer surface and antiparallel at the inner surface. The bottom contact of NWs with Ag paste provides the Ohmic contact interface due to the comparable values of electron affinity of ZnO (4.5 eV) and work function of Ag metal (4.2 eV). However, the top contact of ZnO NWs with Pt-coated Si tip provides the Schottky contact interface. The Schottky contact interface becomes reversely biased at the stretched region of NWs restricting the current flow, while it becomes positively biased at the compressed region allowing the flow of large amount of current. Therefore, the Schottky contact between the metal contact and ZnO NW plays a crucial role for the generation of current through the NG.

After the successful demonstration of self-powered NG concept, researchers started to exploit other piezoelectric materials for NGs which can generate voltage enough to operate the portable electronic devices.

3. Piezoelectric Materials for Nanogenerators

Human body provides continuous energy power sources such as mechanical energy, vibration energy and chemical energy. If these could be converted into electricity, the energy can be used to power the wireless devices and charge the mobile phones. This idea was first demonstrated by Wang and co-workers through the successful conversion of bio-mechanical energy from muscle movement into electricity.[40] Figures 2(a) and 2(b) show the photographs and electrical outputs of ZnO-based NGs generated from finger tapping and hamster movement, respectively.

The operation of portable and implantable devices requires the low power, normally supplied by battery or external source which needs the regular replacement or recharging. In this regard, self-powered NGs would be a good choice for portable electronic device format to find a suitable source for scavenging the continuous power from an environmental source.

3.1 Semiconducting piezoelectric material: ZnO

After the introduction of NG concept, a significant work was carried out by Wang et al. They demonstrated NGs composed of the vertically aligned ZnO NWs, which can be driven by ultrasonic waves.[41] The schematic of NG device is shown in Fig. 3(a). ZnO NWs were grown on sapphire or GaN substrate with the formation of continuous ZnO thin film to connect the bottom of all NWs. Top electrode was prepared by creating the periodic array of trenches on Si wafer, followed by Pt metal deposition. Each individual trench played the same role as AFM tip was used to provide the mechanical deformation to the NWs.[39] Top electrode was positioned on the vertically aligned ZnO NWs with the help of optical microscopy. The distance between top electrode and NWs was optimized by tuning the thickness

© 2013 The Japan Society of Applied Physics

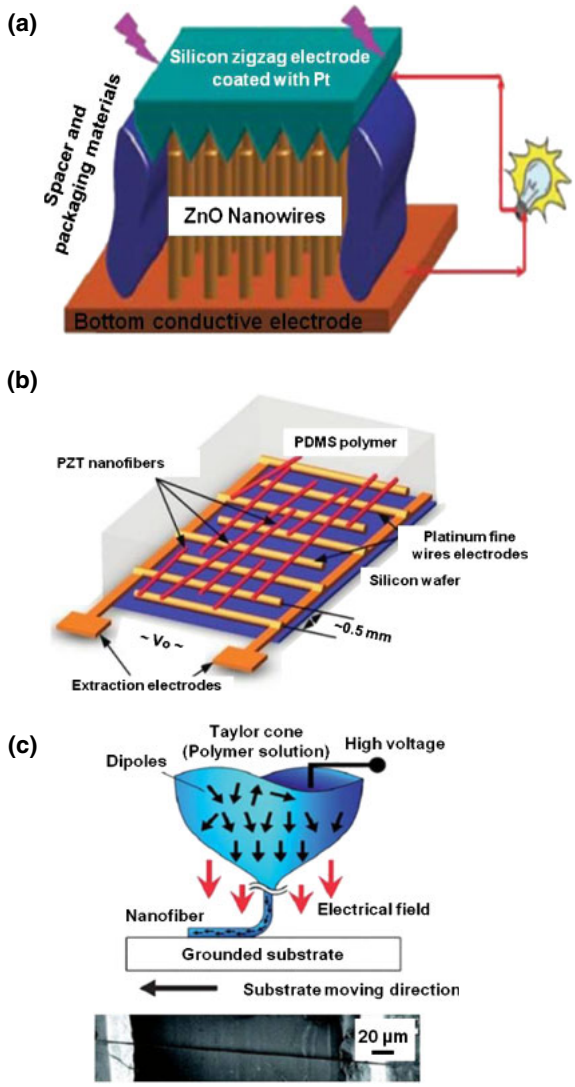

Fig. 3. (Color online) (a) Schematic illustration of ZnO NG device showing the periodic array of trenches on Si wafer followed by Pt metal deposition, used as a top electrode. Individual trench plays the same role as an AFM tip for bending the ZnO NW.[41] (b) Schematic illustration of PZT nanofiber-based NGs device in which interdigitated electrodes are connected to the extraction electrodes for harvesting the charge carriers and a soft polymer PDMS is attached on top of PZT fibers to package the device.[42] (c) Upper part, schematic shows the placing of PVDF nanofibers on the working substrate with in-situ mechanically stretching and poling by utilizing the direct-write technique with the near-field electrospinning process. Lower part shows the measurement of voltage difference between two metallic electrodes.[43]

of polymer film placed at the four corners between top electrode and bottom substrate. Finally, the NG device was mounted on metal plate which was in direct contact with the water contained cavity of an ultrasonic generator. The device was subjected to the ~41 kHz frequency and the output performance was measured using the external circuit. The ultrasonic waves derived the electrodes up and down to bend or vibrate the NWs for simultaneous creation, collection and output of electricity generated by many NWs. The output electricity was reasonably stable and the generated current was continuous when ultrasonic waves were "on" whereas it disappeared when the waves were turned "off". Therefore, the importance of this work was to achieve the continuous output, however, the generated output voltage was 5–10 times smaller than that achieved by deflecting the ZnO NW by AFM tip due to the less vibrations of NWs by ultrasonic waves as compared to deflection created by AFM tip.

3.2 Insulating piezoelectric materials: PZT and PVDF

In addition to ZnO, researchers have started to explore the possibility of NGs based on insulating piezoelectric materials such as $BaTiO_3$ and PZT. In this class of materials, PZT, a perovskite material became one of the most promising candidate due to its excellent piezoelectric properties ($d_{33} = 60$–$130\,\mathrm{pC/N}$) over those of ZnO ($d_{33} = 5.9\,\mathrm{pC/N}$) and other materials. Thus, for a given dimension and energy input, PZT can generate much higher output voltage than other semiconducting piezoelectric materials. Among PZTs with various composition ratios, $Pb(Zr_{0.52}Ti_{0.48})O_3$ near the morphotropic phase boundary (MPB) exhibits excellent ferroelectric and piezoelectric properties, which make it most suitable for applications in NGs. In order to activate the piezoelectric properties of the insulating materials, it is heated up to its Curie temperature. After that, a voltage field with a sufficient strength is applied in the desired direction, forcing the ions to realign along the poling axis. When this material is cooled down, ions maintain their effective orientation along the poling axis. After this poling process, the external strain makes the charge center of dipoles displace and create an accumulation of opposite charges at two ends of material surfaces. Chen et al. reported the PZT nanofibers-based NG to achieve the output voltage of ~1.6 V.[42] PZT nanofibers were prepared by employing the electrospinning synthesis process, which exhibit extremely high piezoelectric voltage coefficient (g_{33}) of $\sim 0.079\,\mathrm{VmN^{-1}}$. The diameter of PZT fibers can be controlled by varying the concentration of poly(vinyl pyrrolidone) (PVP) in sol–gel solution. NG device was fabricated by depositing the PZT fibers of ~60 nm on the interdigitated electrodes made of Pt fine wires. These interdigitated electrodes with diameter of ~50 μm and distance of 500 μm between two adjacent electrodes were assembled on Si substrate. After depositing the PZT fibers on the interdigitated electrodes, annealing process was done at 650 °C for 25 min to get a pure perovskite phase of PZT. The interdigitated electrodes were connected to the extraction electrodes for collecting the charge carriers and a soft polymer, poly(dimethylsiloxane) (PDMS) was attached on top of PZT fibers to package the device. The schematic of complete device is shown in Fig. 3(b). The polling process of PZT nanofibers were performed by applying the electric field of 4 V/μm at 140 °C for 24 h. The as-fabricated NG device can easily be released from Si substrate and integrated on desired flexible substrate. When an alternating pressure was applied perpendicularly to the surface of the device, the outstanding output voltage was produced due to the displacement of charge centers of the dipoles. The nanofiber between two adjacent electrodes is served as single unit which produced the voltage difference. The voltage differences from all such units were added up and finally extracted through the extraction electrodes to get the enhanced output voltage. For good performance, it was desirable that the nanofibers should be laterally aligned to the interdigitated electrodes which can be controlled by

© 2013 The Japan Society of Applied Physics

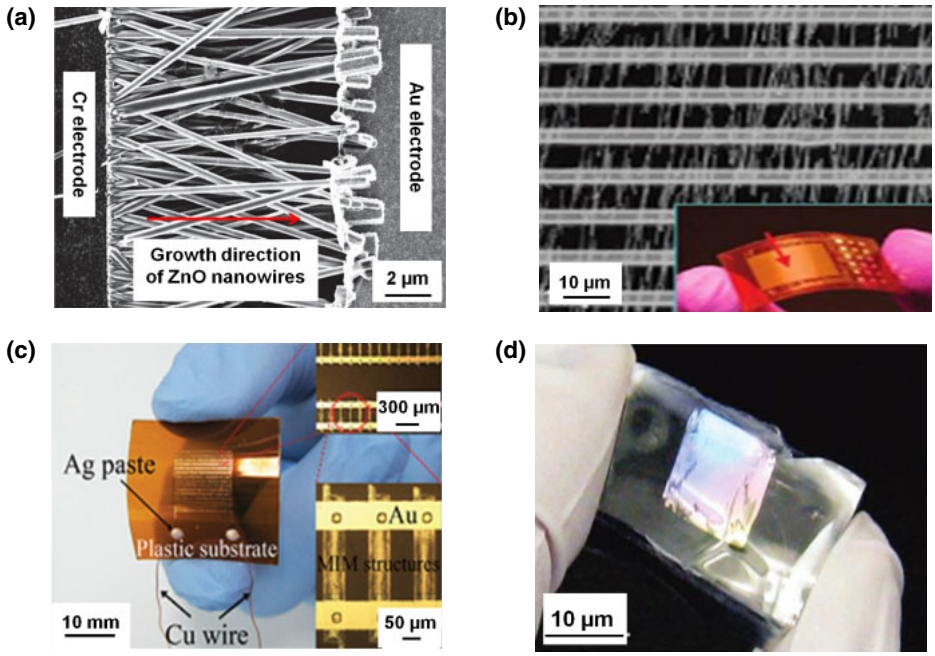

Fig. 4. (Color online) (a) SEM image of ZnO NWs between two electrodes in lateral integration configuration. (b) SEM image of electrode deposited across the horizontally aligned ZnO NWs. Inset shows the photograph of flexible nanogenerator (arrow indicate the effective working area).[45] (c) Photograph of $BaTiO_3$ thin film based NG attached to the plastic substrate. Inset shows the metal–insulator–metal structure connected to the interdigitated electrodes.[46] (d) Photograph of PZT ribbons attached to the rubber like substrate.[47]

optimizing the electric field during the electrospinning of the nanofibers. The maximum output voltage and power output of ~1.6 V and of ~0.6 μW, respectively, was obtained when the top of device was periodically knocked by finger force which is corresponding to the load of ~6 MΩ.

Another class of insulating piezoelectric materials is the piezo-polymer material. The most studied piezoelectric polymer is PVDF with good flexibility, lightweight and biocompatibility. However, it has the relatively low piezoelectric coefficient (~25 pC/N) because of the limitation of the alignment of the H–C–F dipoles and randomly oriented crystals. PVDF have three different crystalline phases of α, β, and γ that should be mechanically stretched and electrically polled to obtain the β phase with good piezoelectricity. Chang et al. demonstrated the PVDF nanofibers-based NGs by utilizing the direct-write technique with the near-field electrospinning process.[43] PVDF nanofibers were placed on the substrate with in situ mechanically stretching and electrical poling process as shown in Fig. 3(c). The advantage of this process is that the electric field of the order of $\sim 10^7$ V/m and stretching force during the electrospinning process can effectively align the dipoles through the phase transition from randomly oriented α phase to polar β phase. The dimension of nanofibers can be controlled in the broad range of diameter (0.5–6.5 μm) and lengths (100–600 μm) [Fig. 3(c)]. The measured voltage and current outputs are 5–30 mV and 0.5–3 nA, respectively.

4. Demand of Flexibility in Nanogenerators

The performance of NG devices degraded gradually due to the occurrence of fracturing/cracks inside the active materials if there is no special device geometry for relaxing the strain. Recently, many efforts have been carried out to fabricate flexible NGs using various piezoelectric materials. Wang and co-workers introduced the new way to enhance the performance of ZnO-based NGs using the large number of vertically and laterally aligned ZnO NWs with flexibility.[44] In case of vertical integration of three layers of ZnO NWs, the output voltage of ~243 mV and current density of ~18 nA/cm^2 are achieved, whereas the ZnO NWs integrated laterally achieves the output voltage and current of ~1.26 V and ~28.8 nA, respectively. Figure 4(a) shows the SEM image of ZnO NWs between two electrodes in lateral integration configuration. Zhu et al. successfully fabricated high-output, flexible NGs using a multiple lateral ZnO NW array by employing a sweeping-printing method.[45] The approach consists of two key steps. First, the vertically aligned ZnO NWs were transferred to receiving substrate and swept to form a laterally aligned array. Second, parallel strips of electrodes were deposited across the NW array. The evenly spaced electrode pattern over the horizontally aligned NWs was defined by employing the photolithography method and then followed by sputter deposition of 300 nm thick Au film. After lifting off the photoresist, 600 rows of stripe-shaped Au electrodes with 10 μm spacing were fabricated on top of the horizontally aligned NW array. Au electrodes form Schottky contacts with the ZnO NWs, which are necessary for a successful operation of NG. Figure 4(b) shows the SEM image of electrode deposited across the horizontally aligned ZnO NWs and inset presents an optical image of flexible nanogenerator. The electrical output of device reached a peak voltage of ~2.03 V, current of ~107 nA, and a peak power density of ~11 mW/cm^3.

In case of single-crystal perovskites, such as $BaTiO_3$ and PZT film, transfer printing process are required to realize the flexible NGs because these materials need the high temperature process which do not allow to fabricate directly on the flexible substrates. Park et al. reported a $BaTiO_3$ thin

© 2013 The Japan Society of Applied Physics

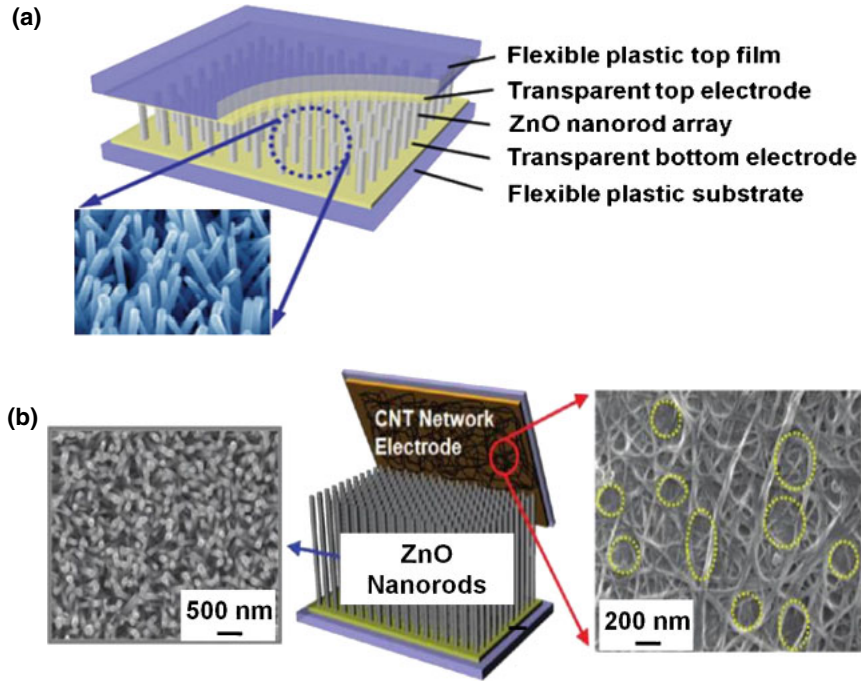

Fig. 5. (Color online) (a) Schematic illustration of vertically aligned ZnO nanorod-based transparent and flexible NG device. Pd/Au and ITO are deposited as top electrode materials on top of ZnO nanorods on flexible substrates. Magnified part shows the SEM image of ZnO nanorods.[49] (b) Middle part shows the schematic of the complete NG device structure using single-walled CNT as top electrode. Left part shows the SEM image of ZnO nanorods and right part shows of network of single-walled CNT as a top electrode.[35]

film based-NG on plastic substrates.[46] First, $BaTiO_3$ was deposited on bulk substrates and annealed at high temperature for crystallization. Then, the film was transferred onto flexible substrates by means of standard micro-fabrication and soft lithographic printing techniques. Figure 4(c) shows the photograph of $BaTiO_3$ thin film-based NG on the plastic substrate. Inset indicates the metal–insulator–metal structure connected to the interdigitated electrodes. The $BaTiO_3$-based NG fabricated on a plastic substrate exhibits an output voltage of ~1.0 V and a current signal of ~26 nA. The output current density and power density were evaluated as ~0.19 $\mu A/cm^2$ and ~7 mW/cm^3, respectively. In addition, PZT is a brittle ceramic with limited mechanical flexibility. McAlpine group reported that the piezoelectric PZT nanoribbons can be fabricated from high quality thin films grown on rigid wafers and subsequently printed onto rubber or plastic sheets using a scalable transfer printing method for flexible energy harvesting system.[47] The transfer technique includes the relocation process of materials from the host inorganic substrate to plastic substrate using PDMS stamps, which has been widely used for transferring micro/nanostructures of inorganic semiconductor onto plastic.[48] As most plastics often melt or deform at temperature range of 100–200 °C, the transfer method became effective tool for inorganic materials which need the high temperature annealing process over 600 °C for crystallization. Before transfer printing, 500 nm thick, 5 mm wide PZT ribbons (10 mm center-to-center spacing) were patterned on the host MgO substrate and then ribbons were comprehensively transferred to the PDMS. A photograph of the resulting "piezo-rubber" chip indicates that the PZT ribbons array was uniformly transferred [Fig. 4(d)]. The transfer yield of the PZT ribbons from MgO to the PDMS was achieved over 95% over an area of 1 cm^2.

5. Integration of Optical Transparency with Mechanical Flexibility

In addition to mechanical flexibility, optical transmittance of device has been a great demand for various biomedical applications and wearable electronics. Choi et al. reported a transparent and flexible NG using the vertically aligned ZnO nanorods.[49] Figure 5(a) shows the complete device structure. To achieve the optical transparency over >90%, indium tin oxide (ITO) was used as electrode and the ZnO nanorod arrays were optimized by controlling the density of seed layer. ZnO nanorods were grown on a flexible plastic substrate using a aqueous solution method.[50] This method has the advantages such as low temperature, large-scale growth, and mass productivity. The resulting device generates an output current density of ~1 mA/cm^2 at a load of ~0.9 kgf. The current density is strongly dependent on the ZnO morphology and work function of the top electrode.

ITO and other conventionally available metallic materials limit flexibility of NGs due to their mechanical brittleness. The conductive material, which has been widely studied as an alternative, is carbon nanotube (CNT) with good optical, mechanical, and electrical properties.[51] Choi et al. investigated transparent and flexible NGs using a networked CNT electrode to improve the stability of device.[35] Figure 5(b) presents the illustration of NG device structure and the SEM images of vertically aligned nanorods and CNT electrode, respectively. The surface morphology of CNT electrode with large pores (>100 nm) can help ZnO nanorods to contact directly CNT electrode under the pushing mode and as a result, allow more nanorods to participate in current generation. Moreover, the low variation in the resistance of

© 2013 The Japan Society of Applied Physics

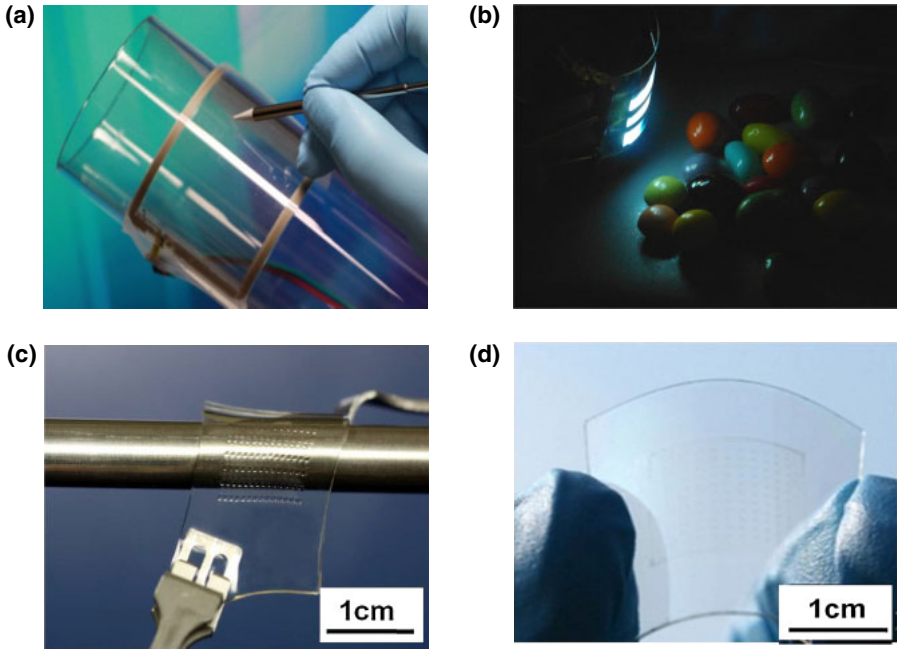

Fig. 6. (Color online) Photographs of (a) touch screen panel using the transparent graphene electrode,[54] (b) OLED lighting device using graphene electrodes on PET substrate,[55] (c) stretchable, printable, and transparent transistors composed of monolithically patterned graphene films,[56] and (d) flexible and transparent transistors using single-walled CNT semiconducting thin films with graphene electrodes.[57]

CNT films during bending tests (<1.1%) support durable, stable, and reliable transparent NGs. The NG with CNT electrode showed transparency of ~84% (at wavelength ~550 nm) and 5 times higher current density than that of ITO-based NG. However, some unfavorable characteristics of CNT such as the difficulty in separating metallic and semiconducting CNTs, diameter dependent electrical properties, and significant roughness, have greatly hindered the performance and development of further applications for CNT-based devices.

6. Graphene: Best Choice for Transparent Flexible Electronics

In recent years, graphene, a one-atom-thick planar sheet of sp^2-bonded carbon atoms densely packed in a honeycomb crystal lattice, has attracted lots of attentions from researchers. The discovery of graphene extracted from graphite using a micromechanical cleavage[52] have allowed the production of high-quality graphene and led to a large range of experimental studies. This two-dimensional (2D) material has opened up new opportunities for various applications such as transistors, light-emitting diodes, solar cells, flexible and stretchable devices.[53] In particular, graphene have been considered as a replacement material for conventional transparent electrode materials such as ITO due to its outstanding electrical and optical properties including high current density, high thermal conductivity, and optical transmittance. The large area, high quality graphene film is needed for practical device applications. Lot of researchers have developed large area growth methods using chemical vapor deposition (CVD). Bae et al. reported the roll-to-roll production of predominantly monolayer 30-in. graphene films grown by CVD on copper substrates and multiple transfer and simple chemical doping methods of graphene films to improve the sheet resistance.[54] The roll-to-roll based approach showed the possibility of the continuous production of graphene films and its applications in electronic devices with large scales such as flexible touch screen [Fig. 6(a)]. The sheet resistance of the synthesized monolayer graphene films was as low as ~125 Ω/sq at optical transmittance of 97%. Furthermore, a chemically doped, four layer film fabricated by a layer by layer stacking process exhibits the sheet resistance of ~30 Ω/sq at transparency of 90%. The result demonstrated that graphene film would be an important alternative to conventional transparent electrode materials.

Another application using graphene transparent electrodes has been demonstrated by flexible organic light-emitting diodes (OLEDs) in 2012.[55] Figure 6(b) shows the photograph of fabricated OLED lighting device using graphene electrodes on poly(ethylene terephthalate) (PET) substrate. Graphene here was synthesized using CVD to get a large-scale and also chemically modified in order to have a high work function and low sheet resistance for good hole injection property. Graphene surface was modified with conducting polymer composition to improve hole injection from the anode to the organic layer and its sheet resistance was reduced to ~40 Ω/sq by doping with p-dopants like HNO_3 or $AuCl_3$. The resulting fluorescent and phosphorescent devices with green color achieved superior luminous efficiencies to those of the devices with an ITO anode. Moreover, white OLED with the graphene anode exhibited a much higher conversion efficiency (CE) (~16.3 cd A^{-1}) than that with the ITO anode (~10.9 cd A^{-1}) and good white electroluminescence spectra with a Commission Internationale de l'Eclairage (CIE) coordinate (0.32, 0.42). These remarkable device efficiencies will demonstrate the great potentiality of graphene as transparent electrodes for flexible organic optoelectronics.

© 2013 The Japan Society of Applied Physics

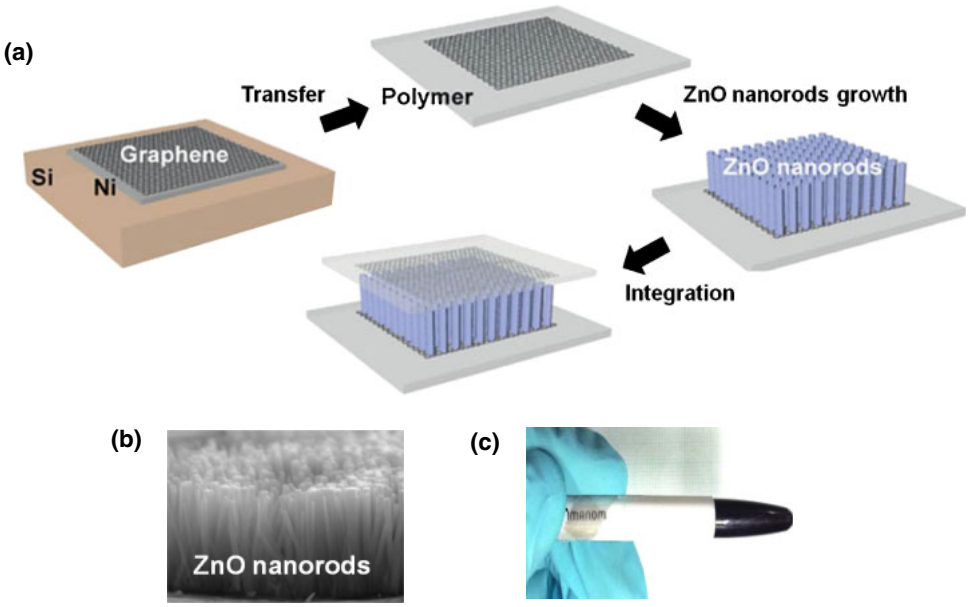

Fig. 7. (Color online) (a) Schematic representation of various fabrication steps of rollable transparent NG. (b) SEM image of vertically aligned ZnO nanorods on graphene films. (c) Photograph of the transparent NG showing its rolling ability.[36)]

Development of stretchable and transparent electronics is one of the biggest issues in electronic devices. For such applications, electronic material should preserve excellent mechanical robustness, electronic functionality, and optical transmittance under a high strain. Graphene film is a promising material for stretchable devices due to its excellent properties. Lee et al. demonstrated stretchable, printable, and transparent transistors [Fig. 6(c)] composed of monolithically patterned graphene films.[56)] The successful demonstration of transistor showed the capability of graphene films as semiconducting channels as well as the source/drain electrodes. Such monolithic graphene transistors showed hole and electron mobilities of $\sim 1188 \pm 136$ and $\sim 422 \pm 52\,\mathrm{cm^2\,V^{-1}\,s^{-1}}$, respectively, with stable operation at stretching up to 5%. Intrinsically stretchable graphene films provide a promising route for creating electrical, optical, and mechanical performance for future stretchable electronic applications which would be difficult to achieve using conventional electronic materials. Jang et al. demonstrated flexible and transparent transistors by utilizing single-walled CNT as semiconducting thin films with graphene electrodes as shown in Fig. 6(d).[57)] The graphene film showed particularly great contact properties with the single-walled CNT channel materials and the resulting devices exhibited a mobility of $\sim 2\,\mathrm{cm^2\,V^{-1}\,s^{-1}}$, On/Off ratio of $\sim 10^2$, transmittance of $\sim 81\%$ and excellent mechanical bendability.

7. Graphene Based Transparent Flexible Nanogenerators

The above discussion shows the potentiality of graphene in realizing the flexible and transparent devices. Furthermore, graphene have been exploited to demonstrate the NG devices which need a stable operation under repeated mechanical stress. In this context, rollable transparent NG enabled by graphene transparent electrodes was demonstrated by Sang-Woo Kim's group in 2010.[36)] Figure 7(a) shows the various fabrication steps of fully rollable transparent NG. Figures 7(b) and 7(c) present the SEM image of vertically aligned ZnO nanorods on graphene films and the photograph of transparent NG with rolling ability, respectively. To accomplish the graphene-based NG, a heterogeneous 3D nanostructure consisting of 1D ZnO nanorods was epitaxially grown on a graphene electrode by a low temperature solution growth. Good electrical conductivity of graphene and its Schottky contact with ZnO nanorods led to the realization of graphene-based NGs with superior charge-scavenging performance. Furthermore, due to the outstanding mechanical properties of the graphene electrode, NGs proved to be electrically and structurally stable under external mechanical loads such as bending and rolling.

Recently, high performance PZT thin film based NGs using graphene as interdigitated electrodes were demonstrated by Kwon et al.[58)] With the extraordinary mechanical, optical and electrical properties of graphene films, the developed PZT based NG showed good flexibility and transparency. Figures 8(a) and 8(b) show the photograph of PZT thin film based flexible NG and a schematic illustration of the fabrication steps of PZT thin film NG with graphene electrode, respectively. To demonstrate power harvesting using PZT piezoelectric ribbons, a transfer method was used to integrate the ribbons onto a plastic with the aid of a thin epoxy layer. First, PZT film was deposited on Si wafer by sol–gel method and annealed at $\sim 650\,^{\circ}\mathrm{C}$ for 30 min for crystallization. After patterning the PZT film to ribbon format, Si wafer was etched in lateral way by dry etching process. PDMS Stamp was attached to PZT ribbons which are floated on the Si wafer after etching process, and transferred to a PET substrate coated with a transparent adhesive. After baking and UV exposure to cure the adhesive, the PDMS stamp was peeled back, leaving PZT ribbons on the PET substrate. Finally, after transfer of graphene film on the top of PZT ribbons, interdigitated

© 2013 The Japan Society of Applied Physics

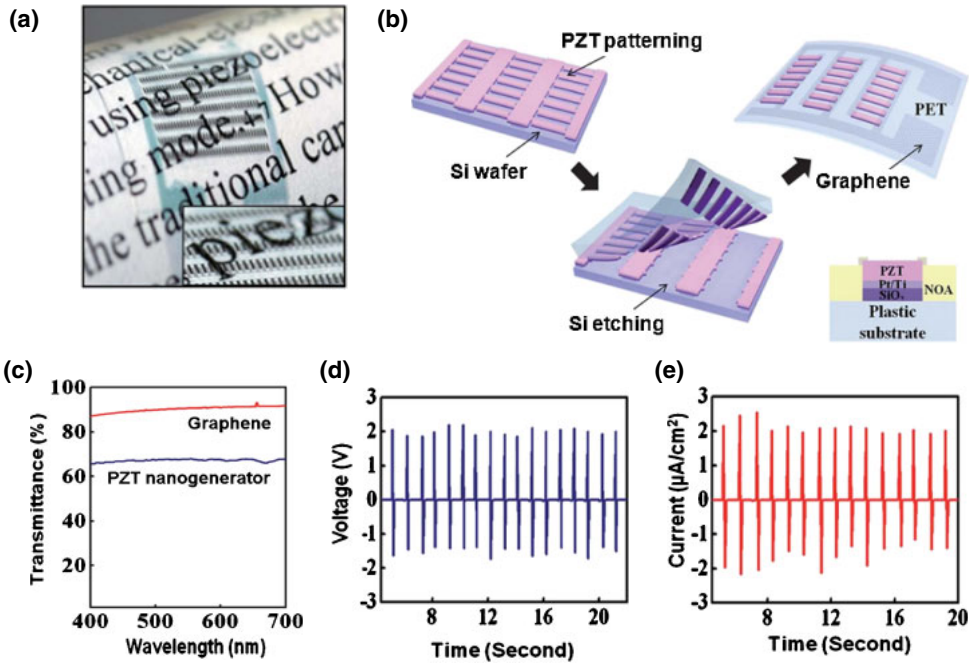

Fig. 8. (Color online) (a) Photograph of PZT based flexible NG. (b) Schematic illustration of the fabrication steps of PZT thin film nanogenerator using graphene electrode. (c) Overall transparency of complete PZT based NG device (~65%). (d) Output voltage and (e) current density generated by PZT based flexible NG.[58)]

Table I. Comparison of various parameters of NGs such as: type of material, shape and size, active area, piezoelectric coefficient (d_{33}), output voltage (V_{out}), output current (I_{out}), current density (J_{out}), and power density (P).

Material	Structure	Substrate	Dimension	Electrode	d_{33} (pm/V)	Output voltage	Output current/current density	Power/ Power Density	Ref.
ZnO	Lateral nanowires	Flexible substrate	D: 200 nm L: 50 μm A: 1 cm^2	Au	14.3–26.7	2.03 V	107 nA	~11 mW/cm^3	45
ZnO	Array of nanowires	PDMS	D: 500 nm L: 6 μm A: 1.5 cm^2	ITO	14.3–26.7	8 V	0.6 μA	~5.3 mW/cm^3	59
PVDF	Nanofibers	Grounded substrate	D: 0.5–6.5 μm L: 0.1–0.6 mm A: /	Metal	−57.6	5–30 mV	0.5–3 nA	2.5–90 pW per cycle (calculated)	22
PZT	Ribbon film	PET film	Ribbon size: 500 μm × 100 μm T: 500 nm A: 60 mm^2	Graphene	250	~2 V	−2.2 mA/cm^2	−88 mW/cm^3	58
PZT	Nanowires	PET film	L: 1.5 cm W: 0.8 mm T: 5 μm A: /	Ag	152	6 V	45 nA	200 $\mu W/cm^3$	60
$BaTiO_3$	Ribbon film	Kapton film	Ribbon size: 300 μm × 50 μm T: 300 nm A: 82 mm^2	Au	30–100	~1 V	0.19 $\mu A/cm^2$	~7 mW/cm^3	46

electrodes perpendicular to the PZT ribbons were formed by photo-resist patterning, and dry etching process of the graphene film. Figure 8(c) shows the overall optical transparency (~65%) of complete PZT-based NG device. Figures 8(d) and 8(e) present the output voltage and current density generated by the PZT-NG. The improvement in NG performance was realized by using the p-type doped graphene, resulting in an increase in current density. NG showed a high output voltage of ~2 V, current density of ~2.2 mA/cm^2 and power density of ~88 mW/cm^3 at an

© 2013 The Japan Society of Applied Physics

applying force of 0.9 kgf, which is enough to run efficiently electronic components in a self-powered mode without any external electrical supply.

Table I summarize various NGs including the type of material, shape and size, active area, piezoelectric coefficient (d_{33}), output voltage (V_{out}), output current (I_{out}), current density (J_{out}), and power density (P).

8. Concluding Remarks

NGs have been intensively studied using various kinds of piezoelectric materials including ZnO, PZT, $BaTiO_3$, and PVDF, and achieved a remarkable development of device performance. For practical applications of NGs, researchers have paid attention to two important issues — high output power voltage and long term mechanical and electrical stability — and made an effort to overcome the limitations. In the context of latter case, graphene has been recognized as one of strong candidates of flexible transparent electrodes which can replace ITO and metal electrodes that result in weak mechanical stability of NGs. Recently, there have been lots of reports on high performance, flexible and rollable NGs enabled by the integration of graphene to various piezoelectric materials. Thus, graphene based NGs would provide an important route to the development of durable energy source for various flexible, stretchable and wearable electronic device applications.

Acknowledgements

This work was supported by the Basic Research Program (2009-0083540 and 2012R1A2A1A03006049) and Global Frontier Research Center for Advanced Soft Electronics (2011-0031635) through the National Research Foundation of Korea (NRF), funded by the Ministry of Education, Science and Technology, Korea.

1) S. R. Anton and H. A. Sodano: Smart Mater. Struct. **16** (2007) R1.
2) H. A. Sadano, D. J. Inman, and G. Park: The Shock Vib. Dig. **36** [3] (2004) 197.
3) J. Chang, M. Dommer, C. Chang, and L. Linn: Nano Energy **1** (2012) 356.
4) Z. L. Wang, X. Wang, J. Song, J. Liu, and Y. Gao: IEEE Prevasive Comput. **7** (2008) 49.
5) B. Kumar and S.-W. Kim: Nano Energy **1** (2012) 342.
6) N. Bu, N. Ueno, and O. Fukuda: Conf. Proc. IEEE Eng. Med. Biol. Soc. **23** (2007) 1362.
7) P. Acevedo Contla and D. K. Das-Gupta: IEEE Conf. Publ. **7** (1991) 917.
8) L. Brown: Biomed. Sci. Instrum. **25** (1989) 119.
9) C. Zuniga, M. Rinaldi, and G. Piazza: IEEE Sens. **11** (2010) 52.
10) K. K. Shung, J. M. Cannata, and Q. F. Zhou: J. Electroceram. **19** (2007) 139.
11) B. Kumar, K. Lee, H. Park, S. J. Chae, Y. H. Lee, and S.-W. Kim: ACS Nano **5** (2011) 4197.
12) Y. Xi, J. Song, S. Xu, R. Yang, Z. Gao, C. Hu, and Z. L. Wang: J. Mater. Chem. **19** (2009) 9260.
13) M. P. Lu, J. Song, M. Y. Lu, M. T. Chen, Y. Gao, L. J. Chen, and Z. L. Wang: Nano Lett. **9** (2009) 1223.
14) Y. Lin, J. Song, Y. Ding, S. Lu, and Z. L. Wang: Appl. Phys. Lett. **92** (2008) 022105.
15) Y. Lin, J. Song, Y. Ding, S. Lu, and Z. L. Wang: Adv. Mater. **20** (2008) 3127.
16) L. Lin, C. Lai, Y. Hu, Y. Zhang, X. Wang, C. Xu, R. L. Snyder, L. Chen, and Z. L. Wang: Nanotechnology **22** (2011) 475401.
17) C. Huang, J. Song, W. Lee, Y. Ding, Z. Gao, Y. Hao, L. Chen, and Z. L. Wang: J. Am. Chem. Soc. **132** (2010) 4766.
18) Z. Huang, Q. Zhang, S. Corkovic, R. Dorey, and R. Whatmore: IEEE Trans. Ultrason. Ferroelectr. Freq. Control **53** (2006) 2287.
19) A. Chaipanich: Curr. Appl. Phys. **7** (2007) 537.
20) H. Lee, R. Cooper, K. Wang, and H. Liang: Sensors **8** (2008) 7359.
21) A. V. Bune, C. Zhu, S. Ducharmeb, L. M. Blinov, V. M. Fridkin, S. P. Palto, N. G. Petukhova, and S. G. Yudin: J. Appl. Phys. **85** (1999) 7869.
22) C. Chang, V. H. Tran, J. Wang, Y.-K. Fuh, and L. Lin: Nano Lett. **10** (2010) 726.
23) Y. Qi, N. T. Jafferis, K. Lyons, Jr., C. M. Lee, H. Ahmad, and M. C. McAlpine: Nano Lett. **10** (2010) 524.
24) E. Siegenthaler, Y. Bochud, P. Wurtz, L. Schmid, and P. Bergamin: J. Usability Stud. **7** [3] (2012) 94.
25) M. R. Bhalla and A. V. Bhalla: Int. J. Comput. Appl. **6** (2010) 3.
26) J. Engel, J. Chen, and C. Liu: J. Micromech. Microeng. **13** (2003) 359.
27) Y. Xu, Y.-C. Tai, A. Huang, and C.-M. Ho: J. Microelectromech. Syst. **12** (2003) 740.
28) H. J. Qi, K. B. K. Teob, K. K. S. Lauc, M. C. Boycea, W. I. Milneb, J. Robertsonb, and K. K. Gleasonc: J. Mech. Phys. **51** (2003) 2213.
29) J.-P. Salvetat, J.-M. Bonard, N. H. Thomson, A. J. Kulik, L. Forró, W. Benoit, and L. Zuppiroli: Appl. Phys. A **69** (1999) 255.
30) R. D. Mansano and A. P. Mousinho: Mater. Sci. Appl. **2** (2011) 381.
31) I. W. Frank, D. M. Tanenbaum, A. M. van der Zande, and P. L. McEuen: J. Vac. Sci. Technol. **25** (2007) 2558.
32) A. R. Ranjbartoreh, B. Wang, X. Shen, and G. Wang: J. Appl. Phys. **109** (2011) 014306.
33) Y. Zhu, S. Murali, W. Cai, X. Li, J. Suk, J. R. Potts, and R. S. Ruoff: Adv. Mater. **22** (2010) 3906.
34) L. A. Falkovsky: J. Phys. **129** (2008) 012004.
35) D. Choi, M.-Y. Choi, H.-J. Shin, S.-M. Yoon, J.-S. Seo, J.-Y. Choi, S. Y. Lee, J. M. Kim, and S.-W. Kim: J. Phys. Chem. C **114** (2010) 1379.
36) D. Choi, M.-Y. Choi, W. M. Choi, H.-J. Shin, H. K. Park, J. S. Seo, J. Park, S.-M. Yoon, S. J. Chae, Y. H. Lee, S.-W. Kim, J.-Y. Choi, S. Y. Lee, and J. M. Kim: Adv. Mater. **22** (2010) 2187.
37) B. K. Sharma, N. Khare, M. Kumar, and P. Kumar: Chem. Phys. Lett. **515** (2011) 62.
38) L. Schmidt-Mende and J. L. MacManus-Driscoll: Mater. Today **10** [5] (2007) 40.
39) Z. L. Wang and J. Song: Science **312** (2006) 242.
40) R. Yang, Y. Qin, C. Li, G. Zhu, and Z. L. Wang: Nano Lett. **9** (2009) 1201.
41) X. Wang, J. Song, J. Liu, and Z. L. Wang: Science **316** (2007) 102.
42) X. Chen, S. Xu, N. Yao, and Y. Shi: Nano Lett. **10** (2010) 2133.
43) C. Chang, V. H. Tran, J. Wang, Y.-K. Fuh, and L. Lin: Nano Lett. **10** (2010) 726.
44) S. Xu, Y. Qin, C. Xu, Y. Wei, R. Yang, and Z. L. Wang: Nat. Nanotechnol. **5** (2010) 366.
45) G. Zhu, R. Yang, S. Wang, and Z. L. Wang: Nano Lett. **10** (2010) 3151.
46) K.-I. Park, S. Xu, Y. Liu, G.-T. Hwang, S.-J. L. Kang, Z. L. Wang, and K. J. Lee: Nano Lett. **10** (2010) 4939.
47) Y. Qi, N. T. Jafferis, K. Lyons, Jr., C. M. Lee, H. Ahmad, and M. C. McAlpine: Nano Lett. **10** (2010) 524.
48) K. Park, D.-K. Lee, B.-S. Kim, H. Jeon, N.-E. Lee, D. Whang, H.-J. Lee, Y. J. Kim, and J.-H. Ahn: Adv. Funct. Mater. **20** (2010) 3577.
49) M.-Y. Choi, D. Choi, M.-J. Jin, I. Kim, S.-H. Kim, J.-Y. Choi, S. Y. Lee, J. M. Kim, and S.-W. Kim: Adv. Mater. **21** (2009) 2185.
50) L. Vayssieres: Adv. Mater. **15** (2003) 464.
51) D. S. Hecht, L. Hu, and G. Irvin: Adv. Mater. **23** (2011) 1482.
52) K. S. Novoselov, A. K. Geim, S. V. Morozov, D. Jiang, Y. Zhang, S. V. Dubonos, I. V. Grigorieva, and A. A. Firsov: Science **306** (2004) 666.
53) D. Shin, S. Bae, C. Yan, J. Kang, J. Ryu, J.-H. Ahn, and B. H. Hong: Carbon Lett. **13** (2012) 1.
54) S. Bae, H. Kim, Y. Lee, X. Xu, J.-S. Park, Y. Zheng, J. Balakrishnan, T. Lei, H. R. Kim, Y. I. Song, Y.-J. Kim, K. S. Kim, B. Özyilmaz, J.-H. Ahn, B. H. Hong, and S. Iijima: Nat. Nanotechnol. **5** (2010) 574.
55) T. H. Han, Y. Lee, M.-R. Choi, S.-H. Woo, S.-H. Bae, B. H. Hong, J.-H. Ahn, and T.-W. Lee: Nat. Photonics **6** (2012) 105.
56) S.-K. Lee, B. J. Kim, H. Jang, S. C. Yoon, C. Lee, B. H. Hong, J. A. Rogers, J. H. Cho, and J.-H. Ahn: Nano Lett. **11** (2011) 4642.
57) S. Jang, S. Jang, H. Jang, Y. Lee, D. Suh, S. Baik, B. H. Hong, and J.-H. Ahn: Nanotechnology **21** (2010) 425201.
58) J. Kwon, W. Seung, B. K. Sharma, S.-W. Kim, and J.-H. Ahn: Energy Environ. Sci. **5** (2012) 8970.
59) L. Lin Y. Hu, C. Xu, Y. Zhang, R. Zhang, X. Wen, and Z. L. Wang: Nano Energy **2** (2013) 75.
60) W. Wu, S. Bai, M. Yuan, Y. Qin, Z. L. Wang, and T. Jing: ACS Nano **6** (2012) 6231.

© 2013 The Japan Society of Applied Physics